Int. J. Solids Structures Vol. 18, No. 9, pp. 819–826, 1982
Printed in Great Britain.

0020-7683/82/090819-08$03.00/0

PLASTIC COLLAPSE OF SQUARE RINGS

D. K. SINHA
Department of Mechanical Engineering, University of Manitoba, Winnipeg, Manitoba, Canada R3T 2N2

and

N. R. CHITKARA
Department of Mechanical Engineering, University of Manchester Institute of Science and Technology, Manchester M60 1QD, England

(*Received* 13 *May* 1981; *in revised form* 1 *December* 1981)

Abstract—Plastic collapse analysis of square rings subjected to in-plane crushing between two opposed indenters is presented. Formulae for the plastic collapse load and the resisting load of the collapsed ring are derived. The plastic collapse load is determined from the stability analysis of the vertical members, treating them as slender columns with initial imperfection and elastic end-constraints and subjected to axial loads. The resisting load of the collapsed ring is found by assuming plastic hinges at mid-points of each of the arms of the ring and a constant "co-efficient of friction" between the tools and the ring surface. Results of experimental observations on the load-tool movement relationship of 3 in. × 3 in. square rings are also given and are shown in good agreement with theoretical predictions, if Tresca's criterion of yield is used.

NOTATION

A area of cross section
E Young's modulus of elasticity
H length of the arms of the square ring
I instantaneous centre of rotation
I_z least moment of area
K factor of initial imperfection
P resisting load
P_2 $= P/2$
P_E Euler load $= \pi^2 EI_z/H^2$
a amplitude of initial imperfection
f distance of extreme fibre from neutral axis
k shear yield stress
p $= \sqrt{(P_2/EI_z)}$
r radius of gyration
t thickness of the ring walls
y deflection of the mid-point of the arms of the ring
y_0 initial imperfection
y_1 deflection due to axial load
y_t $= y_0 + y_1$
Δ relative movement of the indenters (tool-movement)
Δ_{cr} tool-movement at which peak value of the resisting load is observed
α $= \pi/H$
β angle of rotation of the rigid right-angle shaped portions of the ring
μ 'co-efficient of friction'
μ_{max} maximum value of the 'co-efficient of friction'
σ_y initial yield stress of material
σ_E $= P_E/A$
σ $= P/A$
ω instantaneous speed of rotation of the rigid portions of the ring
η $= KH/r$, non-dimensionalised initial imperfection

INTRODUCTION

Plastic collapse analysis of circular metallic rings and tubings in ring mode of deformation, where each cross-section of the tubing material undergoes exactly similar geometrical changes, have been carried out by various authors in the past[1–3]. These studies were prompted, of course, by the fact that circular tubings and rings formed very important structural elements and therefore, for better utilization of these a thorough understanding of their collapse

mechanism was deemed necessary. Circular sections also provide cheap energy absorbing devices and hence theoretical prediction of the resisting load at different stages of plastic collapse has been obtained to estimate their energy absorbing capacity. In recent years the use of square, rectangular and hexagonal tubings has been steadily increasing. It is therefore, proper that studies on similar lines be conducted on these non-circular sections as well. In this paper an attempt is made to obtain plastic collapse load and load-deflection (tool-movement) characteristic for collapsed square thin rings when subjected to in-plane quasi-static compression between two opposed wedge-shape indenters. The plastic collapse load will be determined from the stability analysis of the vertical members of the rings, treating them as slender columns with sinusoidally distributed initial imperfection, to which, elastic end-constraints are provided by the horizontal members and loads in axial direction applied at both ends.

1. DETERMINATION OF COLLAPSE LOAD

Let's assume that the shape of the initially deformed arms of the ring are given by a Sine curve of the following type (Fig. 1):

$$y_0 = a \sin \alpha x \tag{1}$$

where,

$$\alpha = \frac{\pi}{H}$$

Looking at the free-body diagram of a vertical arm in a slightly bent position we can write the following differential equation of the state of equilibrium:

$$EI_z \frac{d^2 y_1}{dx^2} = -P_2 y_t + M \tag{2}$$

where, $y_t = y_0 + y_1$, is the total deflection, and

$$P_2 = P/2 \tag{3}$$

Substituting from eqns (1) and (3) for y_0 and y_t in eqn (2), we have:

$$\frac{d^2 y_1}{dx^2} = -\frac{P_2}{EI_z} - \frac{P_2}{EI_z} a \sin \alpha x + \frac{M}{EI_z}.$$

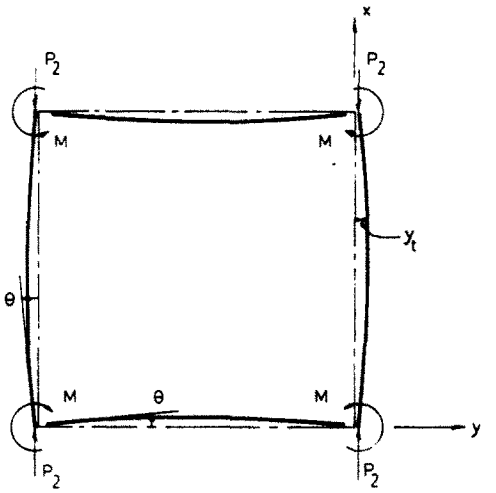

Fig. 1. Free-body diagram of the vertical members of a square ring.

The general solution of the above equation is:

$$y_1 = A\cos px + B\sin px + \frac{a\sin \alpha x}{\alpha^2/p^2 - 1} + \frac{M}{P_2} \tag{4}$$

The constants A and B may be evaluated from the following boundary conditions:

$$y_1 = 0 \quad \text{at} \quad x = 0, H,$$

thus

$$y_1 = \frac{M}{P_2}(1 - \cos px) - \frac{M}{P_2}\tan\frac{pH}{2}\sin px + \frac{a\sin \alpha x}{\alpha^2/p^2 - 1} \tag{5}$$

From eqn (5) we find the expression for the slope as:

$$y_1' = \frac{Mp}{P_2}\sin px - \frac{Mp}{P_2}\tan\frac{pH}{2}\cos px + \frac{a\alpha\cos \alpha x}{\alpha^2/p^2 - 1} \tag{6}$$

At $x = 0$, $y_1' = \theta = (MH/2EI_z)$ or,

$$\frac{MH}{2EI_z} = -\frac{Mp}{P_2}\tan\frac{pH}{2} + \frac{a\alpha}{\alpha^2/p^2 - 1}$$

or,

$$M = \frac{\alpha a P_2 p}{(\alpha^2 - p^2)(pH/2 + \tan pH/2)} \tag{7}$$

The maximum deflection of the vertical arm takes place at the mid-section given by:

$$y_1|_{x=H/2} = M/P_2(1 - \cos pH/2) - M/P_2\tan pH/2\sin pH/2 + \frac{a}{\alpha^2/p^2 - 1}$$

$$= M/P_2(1 - \sec pH/2) + \frac{ap^2}{\alpha^2 - p^2}.$$

And hence the total deflection at the mid-section:

$$y_t|_{x=H/2} = M/P_2(1 - \sec pH/2) + \frac{a\alpha^2}{\alpha^2/p^2 - 1}.$$

Substituting for M from eqn (7) we have:

$$y_t|_{x=H/2} = \frac{a\alpha^2}{(\alpha^2 - p^2)}\left(\frac{p(1 - \sec pH/2)}{\alpha(pH/2 + \tan pH/2)} + 1\right).$$

The above equation can be more conveniently expressed in terms of the Euler load $P_E = (\pi^2 EI_z/H^2)$, thus:

$$y_t|_{x=H/2} = \frac{a}{1 - \dfrac{P_2}{P_E}}\left(\sqrt{\frac{P_2}{P_E}} \times \frac{1 - \sec\dfrac{\pi}{2}\sqrt{\dfrac{P_2}{P_E}}}{\dfrac{\pi}{2}\sqrt{\dfrac{P_2}{P_E}} + \tan\dfrac{\pi}{2}\sqrt{\dfrac{P_2}{P_E}}} + 1\right) \tag{8}$$

If the distance of the extreme fibre of the mid-section from its neutral axis be "f", and $\sigma = P_2/A$, $\sigma_E = P_E/A$; "r" be the radius of gyration and σ_b the stress at the extreme of the

section, we have:

$$\sigma_b = \sigma + \frac{fa}{[1-(\sigma/\sigma_E)]r^2}\left(\sqrt{\frac{\sigma}{\sigma_E}}\frac{1-\sec \pi/2\sqrt{(\sigma/\sigma_E)}}{\pi/2\sqrt{\frac{\sigma}{\sigma_E}}+\tan \pi/2\sqrt{(\sigma/\sigma_E)}}+1\right) \tag{9}$$

Assuming an ideally plastic material with no strain-hardening the maximum value of $\sigma_b = \sigma_Y$. We may define $\eta = fa/r^2$, as a non-dimensionalised factor of initial imperfection. In BS 449 it has also been expressed as $\eta = KH/r$, and the recommended value of $K = 0.003$[6].

2. POST-COLLAPSE ANALYSIS

2.1 *Determination of the resisting load*

A square ring which is subjected to in-plane compression between two parallel plates or indenters, Fig. 2, may collapse ideally by formation of four hinges at the mid-sections of its arms, so that a viable mechanism allowing movement is created. If it is assumed that the centre of the ring remains stationary and the indenting tools (plates) advance equal distances towards each other a situation like that shown in Fig. 3 would soon arise. We assume that each right-angle shaped portion of the ring between the hinges undergoes rigid rotation with angular speed ω in the respective sense shown in Fig. 3 about instantaneous centres I. It can be seen clearly that due to the horizontal arms caving in, the contact between the indenting tools and the horizontal arms is no longer uniform, it may therefore, be assumed that the applied load (P) is now split up into two concentrated loads each of magnitude ($P/2$) acting at the corners of the ring. We may further assume frictional forces $\mu P/2$, where μ is the "co-efficient of friction" to be explained in sub-section 2.2, acting at the points of contact and in the directions shown in Fig. 3. A free-body force diagram of a quarter of the ring is shown in Fig. 4.

From simple geometrical consideration in Fig. 4 it can be seen that the deflection (y) of the mid-points of the arms of the ring is given as:

$$y = (H/2)\sin\beta \tag{10}$$

and the relationship between the angle of rotation (β) of the arms and the relative tool-

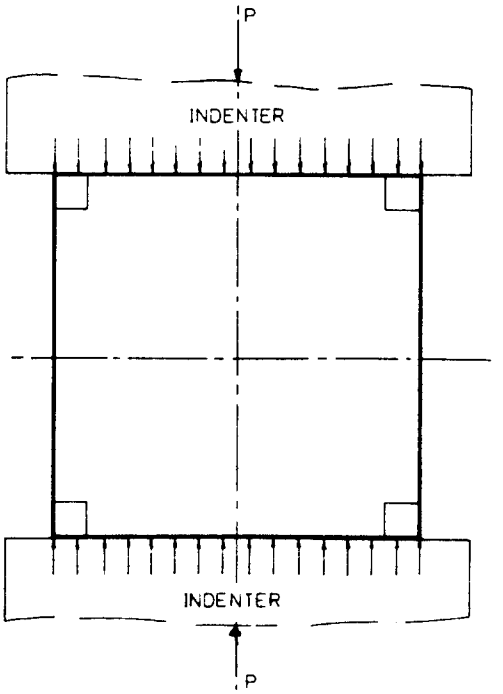

Fig. 2. Initial load-distribution in a square ring subjected to in-plane compression between two rigid indenters.

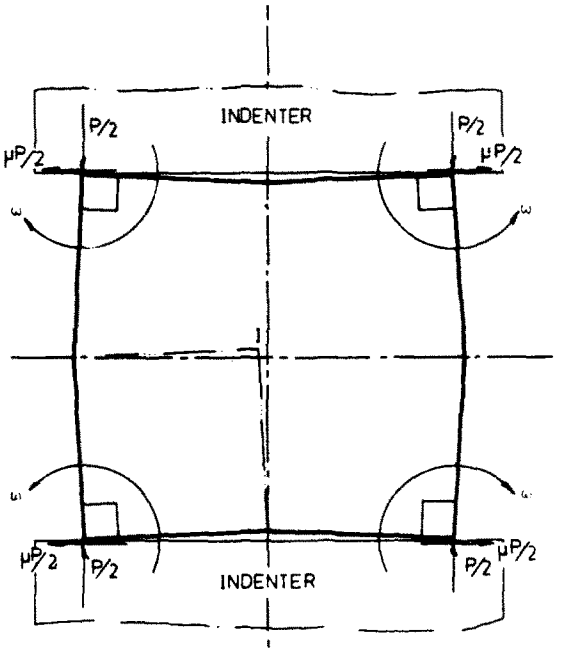

Fig. 3. Collapse mechanism of a square ring.

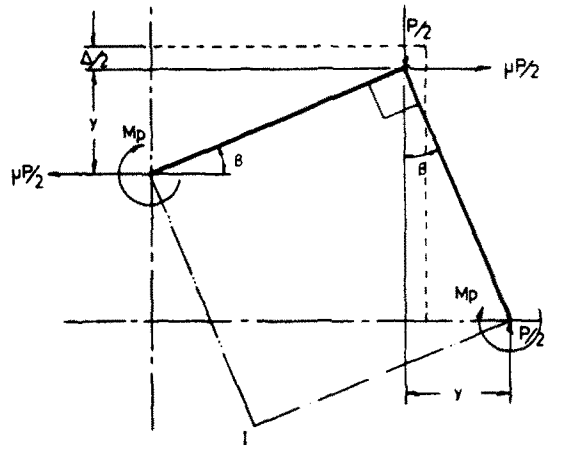

Fig. 4. Free-body force diagram of a quarter of a square ring.

movement (Δ) may be found thus:

$$\Delta/2 = H/2 - H/2 \cos \beta,$$

or

$$\cos \beta = 1 - \Delta/H$$

or

$$\sin \beta = [1 - (1 - \Delta/H^2]^{1/2}. \tag{11}$$

Equating the work done by the external force with the work done by the internal resisting forces and the frictional force we obtain:

$$P/2 \times y \times \omega = \mu \times P/2 \times y \times \omega + 2M_p \times \omega \tag{12}$$

where $M_p = \sigma_y \times t^2/4$, is the plastic-moment per unit length of the ring material. From the eqn (12) above the expression for the resisting load sustained by the ring at the relative tool-

movement (Δ) may be found as:

$$P = \frac{8M_p}{H} \times \frac{1}{(1-\mu)[1-(1-\Delta/H)^2]^{1/2}} \tag{13}$$

2.2. *Determination of the co-efficient of friction*

In the analysis given above it is possible to use a constant value for μ, the 'co-efficient of friction' as applied in metalworking theory. In operations such as extrusion, drawing etc., the tangential stress between the surfaces of the workpiece and the tool or the die is assumed to be directly proportional to the normal stress, thus a "co-efficient of friction" analogous to that used in elementary physics can be applied in all these metal working methods. The tangential stress is however, limited to a value equal to the shear yield stress k of the metal itself[5]. As the least value of the normal stress which causes plastic flow is σ_y, the maximum value of the co-efficient of friction for full sticking friction conditions is given by the ratio k/σ_y.

If von Mises criterion of yielding of the material of the ring is assumed, the shear yield stress and the uniaxial yield stress are related by the following expression:

$$2k = 1.55\sigma_y,$$

thus

$$\mu_{max} = \frac{k}{\sigma_y} = 0.5775. \tag{14}$$

Similarly, if the Tresca yield criterion is assumed we get:

$$2k = \sigma_y$$

or,

$$\mu_{max} = 0.5. \tag{15}$$

Both these values of μ_{max} will be used in Section 2 to compare the theoretical predictions with the experimental results. The reason for adoption of the maximum values of the "co-efficient of friction" in the present discussion follows from the fact that no lubrication was provided between the indenting-tools and the rings and therefore, a condition of "sticking friction"[5] could be assumed such that only possible relative movement was due to shearing of the metal. A justification for the above assumption was, indeed, the presence of extensive shearing of the ring surface at the zones of contact with the indenting tools in all the cases of in-plane compression test.

3. RESULTS

In order to check the validity of predictions made by eqns (9) and (13) for the plastic collapse loads and the resisting load in the post collapse configurations, experimental load-tool deflection relationships were obtained for several sizes of square rings[4]. Set of two load-tool deflection curves for steel rings of size 3 in. × 3 in. square × 0.160 in. (8 SWG) wall thickness and heights $\frac{1}{2}$ in. or 1 in. are being given here. The mechanical properties of the steel were determined experimentally as:

$$E = 30 \times 10^6 \text{ psi}$$
$$\sigma_y = 46{,}000 \text{ psi, and hence}$$
$$M_p = \frac{\sigma_y \times t^2}{4} = 294 \text{ in-lbf/in.}$$

The ring under investigation was placed vertically between two wedge-shaped opposed steel indenters with rounded nose (radius $\frac{1}{4}$ in.). The wedges were guided to move freely in the

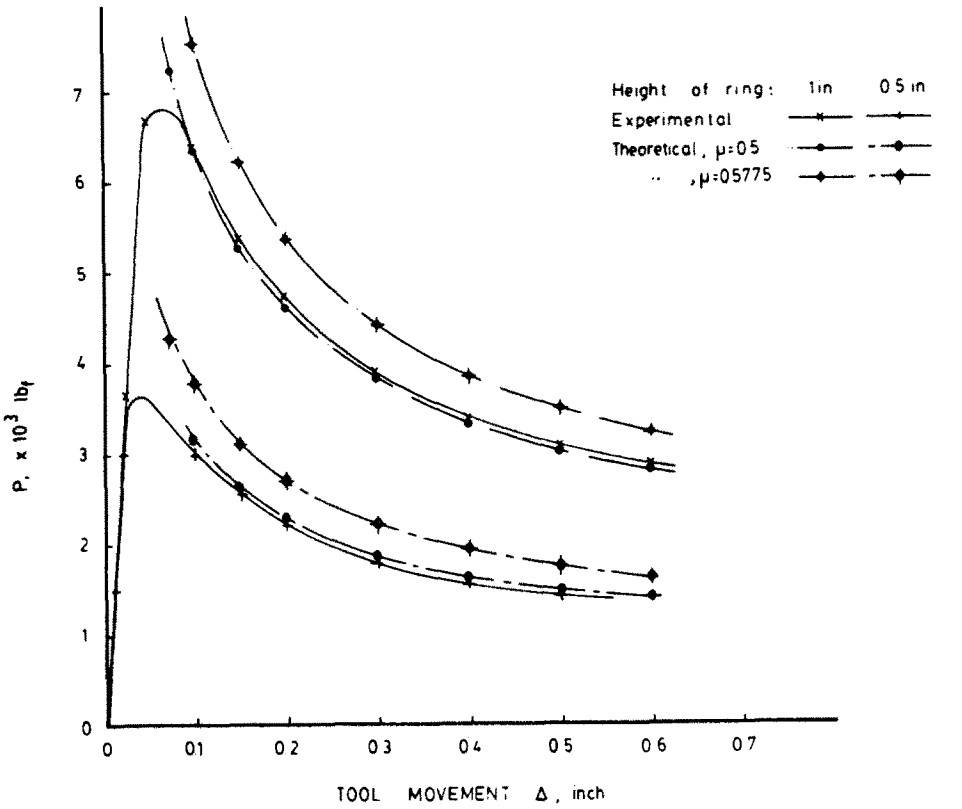

Fig. 5. Load vs tool-movement relationship in 3 in. × 3 in. square rings. Material:—Steel.

vertical direction. The experiment was performed in an "Avery" testing maching. Load was applied very gradually through the indenters and the corresponding relative movement of the indenters recorded accurately. The experimental results were then plotted as smooth curves shown in Fig. 5, in which the tool-movement is the relative movement of the indenters towards each other.

In Fig. 5 are also shown plotted the load-tool *movement* relationship for the $\frac{1}{2}$ in. high and 1 in. high rings obtained from eqn (13). In one set of these theoretical predictions the value of "co-efficient of friction" μ was taken as 0.5 as derived in eqn (15) and in the second set of predictions $\mu = 0.5775$ was used as derived in eqn (14).

In the two instances of $\frac{1}{2}$ in. and 1 in. high square rings subjected to in-plane compression a sharp peak load was observed at a small tool-movement (Δ_{cr}). The load in each case then started to drop gradually at higher tool-movements and at large tool-movements of 0.6 in. and above it levelled off to a value nearly $\frac{1}{3}$ the peak load.

As can be seen the theoretical load-tool deflection curves for $\mu = 0.5$ follow the drooping part of the curve quite closely. At tool-movements lower than Δ_{cr} however, there are wide discrepancies between the theoretical and the experimental values of the load. Equation (13) predicts for P an infinite value at $\Delta = 0$, and generally much higher values at all tool-movements lower than Δ_{cr}. This deviation from the observed result is due to the fact that at tool-movements lesser than Δ_{cr}, plastic hinges, the existence of which was assumed in the derivation of eqn (13) are not present. The instant of complete formation of the plastic hinges coincides with the instant of collapse of ring i.e. when the peak value of the resisting load is attained, and therefore only at values of tool-movements higher than Δ_{cr} does eqn (13) become applicable. The estimate of the peak load or the plastic collapse load is determined first by evaluating, iteratively, that value of the axial compressive stress (σ) which will cause incipient plasticity to set-in at the extreme fibres of the mid-section of the arms of the ring, i.e. $\sigma_b = \sigma_Y$. The peak load is then evaluated by simply multiplying σ with the cross sectional area of the arms.

3.1 *Collapse load*

(a) *Ring of height* 1 in.

$$P_E = \pi^2/3^2 \times 30 \times 10^6 \times 1/12 \times (1.6)^3 \times 10^{-3} = 1123.8 \text{ lb}_f$$

$$\sigma_E = 7\,023.5 \text{ lb}_f/\text{in.}^2$$

$$\sigma_Y = 46\,000 \text{ lb}_f/\text{in.}^2$$

$$\eta = 0.003 \times 3/0.046 = 0.19485$$

Solving eqn (9) with the above values of the parameters we find $\sigma = 24\,000 \text{ lb}_f/\text{in.}^2$, from which $P = 7680 \text{ lb}_f$. This estimate of the collapse load is about 13.8% higher than the value shown in Fig. 5.

(b) *Ring of height* $\frac{1}{2}$ in.

The theoretical value of the collapse load for the $\frac{1}{2}$ in. wide ring would be $P = 3840 \text{ lb}_f$, which is about 5.2% higher than the experimentally observed value.

4. CONCLUSIONS

From the theoretical results given in sub-section 3.1 it is seen that in the case of a ring of height $\frac{1}{2}$ in. a very accurate estimate of the collapse load is obtained from the stability analysis, the accuracy, however, diminishes somewhat when the height of the ring is increased to 1 in. This is to be expected from the phenomenon reported in [4] where it is mentioned that the mode of deformation of rings changes continuously as their height is increased. Whereas, in the case of a ring of short height every cross section undergoes exactly similar geometrical changes, this is not exactly true in the case of a ring of higher height. The sections farther away from the loaded cross section undergo lesser and lesser changes. The equation (5) therefore, overestimates the extent of deformation of the cross sections farther away which results in a higher estimate of the plastic-collapse load for the 1 in. high ring.

The post-collapse analysis, based on the assumption of existence of yield hinges at mid-points of the arms of the ring and a constant "co-efficient of friction" akin to that used in metalworking, gives accurate values for the resisting loads sustained by the ring. In authors' opinion the analysis presented here is capable of predicting still more accurate results if the rigid-perfectly plastic model is replaced by a rigid-linearly hardening material model.

Acknowledgements—The experimental work reported herein was carried out within the Applied Mechanics Division of the University of Manchester Institute of Science and Technology, England. The authors wish to express their gratitude to the authorities of the Division for making available the facilities needed for the research and to the management of Tata Steel, India for financial support and leave of absence to the first author.

REFERENCES

1. J. A. DeRuntz and P. G. Hodge, Crushing of tubes between parallel rigid plates. *J. Appl. Mech* **85**, 391 (1963).
2. L. D. Mutchler, Energy absorption of aluminum tubings, 82, 740 (1960).
3. W. Johnson, The compression of circular rings. *J. Ray Aero. Soc.* **60**, 484 (1956).
4. D. K. Sinha, Plastic collapse of thin-walled square and rectangular tubes in transverse loading. M.Sc. Dissertation, University of Manchester Institute of Science and Technology, England (1978).
5. G. W. Rowe, *An Introduction to the Principles of Metalworking*, Arnold, London (1968).
6. British Standard 449: Use of Structural Steels in Building.